frontiers | Frontiers in Earth Science

TYPE Original Research
PUBLISHED 21 August 2024
DOI 10.3389/feart.2024.1453178

OPEN ACCESS

EDITED BY
Chong Xu,
Ministry of Emergency Management, China

REVIEWED BY
Huajin Li,
Chengdu University, China
Jian Ji,
Hohai University, China
Junjun Ni,
Hong Kong University of Science and Technology, Hong Kong, SAR China

*CORRESPONDENCE
Xia Bian,
xia.bian@hhu.edu.cn

RECEIVED 22 June 2024
ACCEPTED 07 August 2024
PUBLISHED 21 August 2024

CITATION
Tao W, Wen Y, Bian X, Ren Z, Xu L, Wang F and Zheng H (2024) Analysis of ecological prevention and control technology for expansive soil slope.
Front. Earth Sci. 12:1453178.
doi: 10.3389/feart.2024.1453178

Analysis of ecological prevention and control technology for expansive soil slope

Wenbing Tao[1], Yingwen Wen[2,3], Xia Bian[4]*, Zhilin Ren[4], Long Xu[5], Fei Wang[1] and Hu Zheng[6]

[1]Anhui Transport Consulting and Design Institute Co. Ltd., Hefei, China, [2]School of Civil Engineering and Architecture, Jiangsu University of Science and Technology, Zhenjiang, China, [3]East China Electric Power Design Institute Co., Ltd., Shanghai, China, [4]Key Laboratory of Ministry of Education for Geomechanics and Embankment Engineering, Hohai University, Nanjing, China, [5]Hefei University of Technology, Hefei, China, [6]Department of Geotechnical Engineering, College of Civil Engineering, Tongji University, Shanghai, China

For the expansion soil slope in the JiangHuai area before the disposal of the neglect of expansion of the weak defects and slope disposal after the poor long-term stability of the current situation. This study investigates the ability of ecological slope protection technology to cope with the destabilizing geohazard of expansive soil slopes. Analyzing the collapse reasons of weak expansive soil slopes in the JiangHuai region based on the reinforcement project of expansive soil slopes along highways in the JiangHuai region, combined with actual engineering research, a "storage-resistance" water regulation ecological prevention and control technology is proposed. The feasibility and sustainability of the ecological slope protection technology is discussed in terms of its principles and influencing factors, and the protection effect is verified by combining numerical simulation and field test methods. Research findings suggest that the "storage-resistance" technology effectively prevents rainwater infiltration, particularly under light rain conditions, with continuous blocking capability. Under rainstorm conditions, it can prevent infiltration for about 4 h, significantly enhancing slope stability. Slope rate variations show no significant impact on reinforced slope stability, with maximum deformation occurring at the slope's foot after rainfall. Reinforcement plans should prioritize strengthening support at the slope's base. Proper selection and optimization of technical parameters can lead to more economical and sustainable solutions while extending protection time. Field trials confirm the suitability of the "storage and blocking" water regulation ecological control technology for the JiangHuai region, particularly where light rain prevails. These findings suggest that ecological control techniques for expansive soil slopes can effectively regulate slope moisture changes and reduce the geohazard risk of expansive soil slope instability.

KEYWORDS

capillary block, jianghuai region, weak expansive soil, ecological control, slope reinforcement

1 Introduction

Slopes, as a common terrain in nature, may be affected by tectonic activities, climate change, and human activities that may result in destabilization and landslide hazards, which poses a serious threat to local communities and infrastructures (Feng et al., 2023; Cai et al., 2024). Studies on the probability of occurrence of georisks have shown that the sensitivity of slopes to various influencing factors varies due to the existence of a multiplicity of soil materials (Ji et al., 2022; Ji and Wang, 2022; Hu et al., 2023; Bian et al., 2024a). This puts higher demands on protective measures to cope with slope destabilization hazards. Expansive soil is a unique soil type with complex engineering properties, exhibiting typical traits of water absorption and expansion, as well as water loss and contraction (Pei et al., 2020; Zhang et al., 2020). When compared to ordinary slopes, the mechanism behind the deformation and destabilization of expansive soil slopes becomes more intricate. In addition to the conventional factors influencing slope stability, it becomes imperative to consider the impact of the expansive soil's inherent properties on slope stability (Zhou et al., 2016; Cai et al., 2019; Xu, 2020; Guo and Zhao, 2021).

The current management practices for expansive soil slopes rely on established experience and standards (Kong and Chen, 2012). Common measures for treating expansive soil slopes include support structure protection, geogrid slope protection, and expansive soil curing treatments. Engineering decisions often consider slope height and utilize passive soil pressure to reduce overturning moments. For slopes exceeding certain heights, schist skeleton slope protection structures are employed to enhance slope stability (Wang et al., 2008; Xian et al., 2017; Zheng et al., 2017). However, over the long-term service life, the rainfall-evaporation process exacerbates crack development in expansive soil (Liu and Yin, 2010; Wang et al., 2016; Chang et al., 2021), potentially leading to superficial and shallow sliding of slopes. This can result in problems such as the overturning of supporting structures, undermining the long-term effectiveness of expansive soil slopes. Geosynthetics have been extensively used as roadbed reinforcement materials globally, combining with soil, stone, or concrete to protect slopes or riverbeds from erosion (Bian et al., 2023). While this method can mitigate slope rates and increase slope stability in expansive soil, its application is limited in regions like JiangHuai, where high rainfall intensity exacerbates the fissuring and expansion/contraction properties of expansive soil (Hu et al., 2007; Wang et al., 2007; Gong and Tong, 2009; Ding and Lei, 2010). In railroad, water conservancy, and highway construction, chemical improvement of expansive soil using materials such as lime and cement has been employed. Treated expansive soil forms a gray covering layer on the surface, effectively reducing expansion potential, enhancing strength, and improving slope resistance to erosion, thus increasing slope stability (Yang et al., 2011). However, due to insufficient volcanic ash reaction of lime and cement and their susceptibility to deterioration upon contact with water, challenges arise in meeting long-term maintenance requirements and economic performance indicators, particularly in large-scale engineering applications.

Expansive soils in the JiangHuai region predominantly consist of medium and weakly expansive soils, which are often overlooked by engineers during disposal processes. While initial engineering stability may appear satisfactory, frequent landslides occur in expansive soils in the JiangHuai region as the rainfall-evaporation process progresses (Duan et al., 2019; Deng et al., 2020; Wei et al., 2021). As understanding of the unique engineering characteristics of expansive soils deepens, the principle of remediation—favoring appropriate retaining soil over clearance, and appropriate drainage over blocking—has become widely accepted. The concept of flexible prevention and control, such as "moisture seepage control, softening to control swelling, and ecological slope protection," is gradually gaining traction. Simultaneously, with increased environmental awareness and the promotion of sustainable development, ecological slope protection has become a focal point of slope protection projects globally. In the study of long-term stability of expansive soil slope protection. Continuous monitoring of geogrid-reinforced repaired expansive soil slopes has shown that geogrid reinforcement can inhibit crack development and limit soil deformation (Zhang et al., 2024). In addition, in terms of resource and energy consumption, flexible slope protection technology has additional environmental benefits compared with chemical improvement technology (Zhang et al., 2019; Zhang et al., 2022). In the process of reinforcing expansive soil slopes in the JiangHuai area, ecological slope protection technology began to be combined with the traditional soil replacement slope protection technology through the improvement of the vegetation growth environment (Gong et al., 2023; Song et al., 2023). Through the introduction of ecological slope protection technology, the slope's anti-infiltration capacity has been improved, and at the same time, additional soil and water conservation capacity can be obtained (Ng et al., 2019; Ng et al., 2022; Ma et al., 2023; Ng et al., 2023). Current landslide management technology for expansive soil still relies heavily on traditional slope management methods, neglecting the issue of landslides caused by crack development due to moisture changes. However, new prevention and control technologies aimed at mitigating water sensitivity and fissuring in expansive soil, as well as enhancing slope body drainage, have been rarely reported. Additionally, research on the ecological protection mechanisms for expansive soil slopes remains relatively undeveloped. Therefore, the proposition of a novel ecological control technology capable of regulating moisture changes in expansive soil slopes is necessary.

The primary objective of this study is to cope with the geologic disaster of expansive soil slope instability, and to study the ecological prevention and control technology of expansive soil slopes that can regulate the moisture change of slopes. Based on the special geological and climatic characteristics of the JiangHuai region, which lead to the instability of expansive soil slopes, this study proposes the ecological control technology of "storage-resistant" moisture regulation of expansive soil slopes. The feasibility and sustainability of the ecological slope protection technology are discussed in terms of the principles and influencing factors, and the protective effect is verified by numerical simulation and field test methods.

2 Overview of expansive soil slope construction in the JiangHuai region

2.1 Slope location and meteorological conditions

The G40 Shanghai-Shaanxi Expressway section from Hefei to Dagudian (referred to as the HeLiuYe Expressway) serves as a crucial thoroughfare connecting Anhui Province with neighboring provinces and municipalities. Spanning Hefei City and Lu'an City within the economic zone along the river in Anhui Province, the project traverses undulating terrain and intermittent valleys. The average precipitation along the route ranges from 989.3 to 1,153.6 mm annually, with the majority occurring from June to August, constituting over 50% of the total annual precipitation.

2.2 Geological condition

The project area's stratum primarily consists of powdery clay from the fourth geological system, with a thickness ranging from 4.0 to 18.0 m. The clay exhibits hard plastic and hard states and contains a minor amount of ferromanganese nodules. Columnar joints are prevalent, and the mineral composition is predominantly composed of hydrophilic minerals such as montmorillonite, ilmenite, and kaolinite.

One hundred sets of soil samples were collected from the HeLiuYe Expressway site, and their free swell characteristics were assessed through macroscopic observation and independent testing. Specifically, the testing of the free swell of the soil samples was conducted according to the Chinese Standard (GB/T 50123-2019, MWR, 2019) (MWR Ministry of Water Resources the People's Republic of China, 2019). Based on the test outcomes, the soil samples were analyzed and classified, with the results depicted in Figure 1, showcasing a free swelling rate range of δ_{ef} = 30.5%–59.0%. The majority of soil samples along the project route exhibit expansion rates below 50%, with only 30% displaying rates exceeding 50%. This suggests that the soil layer predominantly comprises weakly to moderately expansive soils deposited in the Upper Pleistocene of the Quaternary System. Weakly expansive soils prevail, with a minority of moderately expansive soils present.

2.3 Potential engineering issues

In the JiangHuai region, the expansion potential of expansive soil is often underestimated by engineering design and construction personnel. Consequently, effective slope protection measures tailored to the soil's expansion characteristics are frequently overlooked. As a result, the moisture fluctuations in the slope body triggered by rainfall and evaporation processes induce deformation, contraction, and fissure development in expansive soil slopes along riverbanks. Particularly during summer, prolonged dry and wet cycles exacerbate crack formation, leading to extensive development. This can create new water infiltration channels, and subsequent rainfall events may render reinforcement measures ineffective. As a consequence, shallow landslides in expansive soil slopes worsen, leading to destabilization and damage in deeper sections of the slope, as illustrated in Figure 2.

3 Stability analysis of ecological protection for expansive soil slopes

3.1 Numerical modeling

The rainwater infiltration process of ecologically protected expansive soil slopes under various rainfall intensities and slope rates was analyzed using the slope stability analysis and stress-seepage coupling module of the finite element software Midas/gts. Expansive soil slope models with dimensions of 6.0 m in length, 7.0 m in height, and slope rates of 1:0.8, 1:1, 1:1.25, and 1:1.5 were established, as depicted in Figure 3. Based on investigation results, the left node head of the slope model was set at 5 m, and the right node head at 3 m. Rainfall in the JiangHuai region typically consists of prolonged light rain with occasional sudden short-term rainstorm. For the analysis, the rainfall intensity under rainstorm conditions was assumed to be 300 mm/d, with a duration of 5 h, while the intensity for light rainfall conditions was set at 20 mm/d, with a duration of 20 h. When rainfall intensity exceeds the slope's permeability, a portion of the rainwater infiltrates into the slope, while the remainder is lost along the surface. Conversely, when rainfall intensity is lower than the slope's permeability, infiltration is treated as surface flow.

The soil parameters for the slope model were derived from indoor geotechnical tests and engineering survey reports, with specific values detailed in Table 1. The slope soil is simulated using the M-C constitutive model, while slope stability calculations employ the Strength Reduction Method (SRM) to determine the slope's safety coefficient.

3.2 Pore water pressure analysis of slopes

As rainwater infiltrates, the pore water pressure within the slope's soil undergoes changes. The pore water pressure to the slope water table line as the critical line: below this line, the soil is saturated, resulting in positive pore water pressure; above the water table line, the soil is unsaturated, and matrix suction causes negative pore water pressure. With continuous rainwater infiltration, the slope's soil gradually saturates, transitioning the pore water pressure from negative to positive values.

Upon comparison of Figures 4, 5, it is evident that the "storage-blocking" moisture control ecological prevention and control technology effectively regulates pore water pressure distribution. During rainstorm conditions, particularly from rainfall durations of 1 h–3h, pore water pressure exhibits minimal variation, indicating limited infiltration into the slope interior. However, as rainfall persists, especially during the 4th hour, pore water pressure increases gradually, penetrating deeper into the slope, signifying breakthrough of the fine grain layer and subsequent infiltration into the slope's interior. By the 5th hour of rainfall, the saturated area of the slope expands further, with rainwater infiltration extending from the slope's periphery towards its deeper sections, affecting a significant portion of the slope. Conversely, under light rainfall

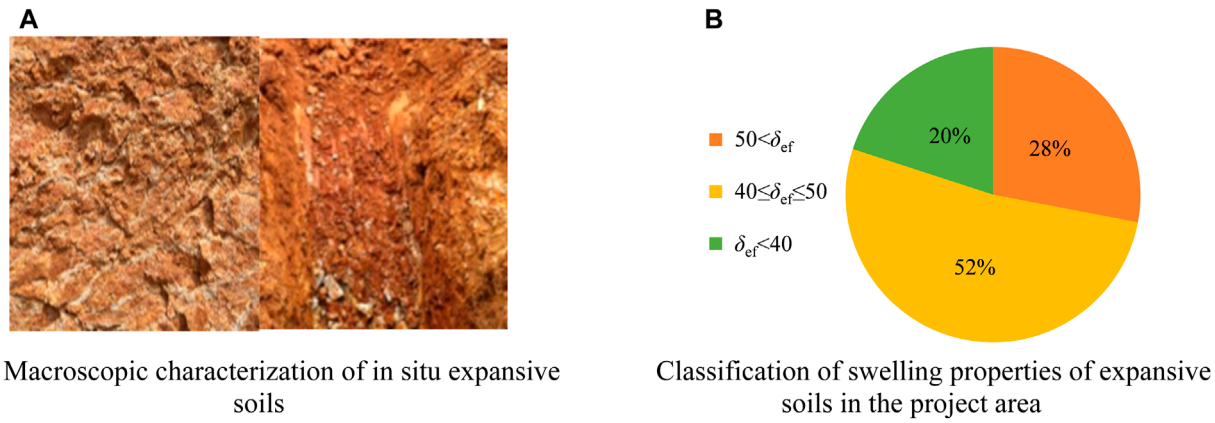

FIGURE 1
Physical characterization of field soil samples. **(A)** Macroscopic characterization of *in situ* expansive soils. **(B)** Classification of swelling properties of expansive soils in the project area.

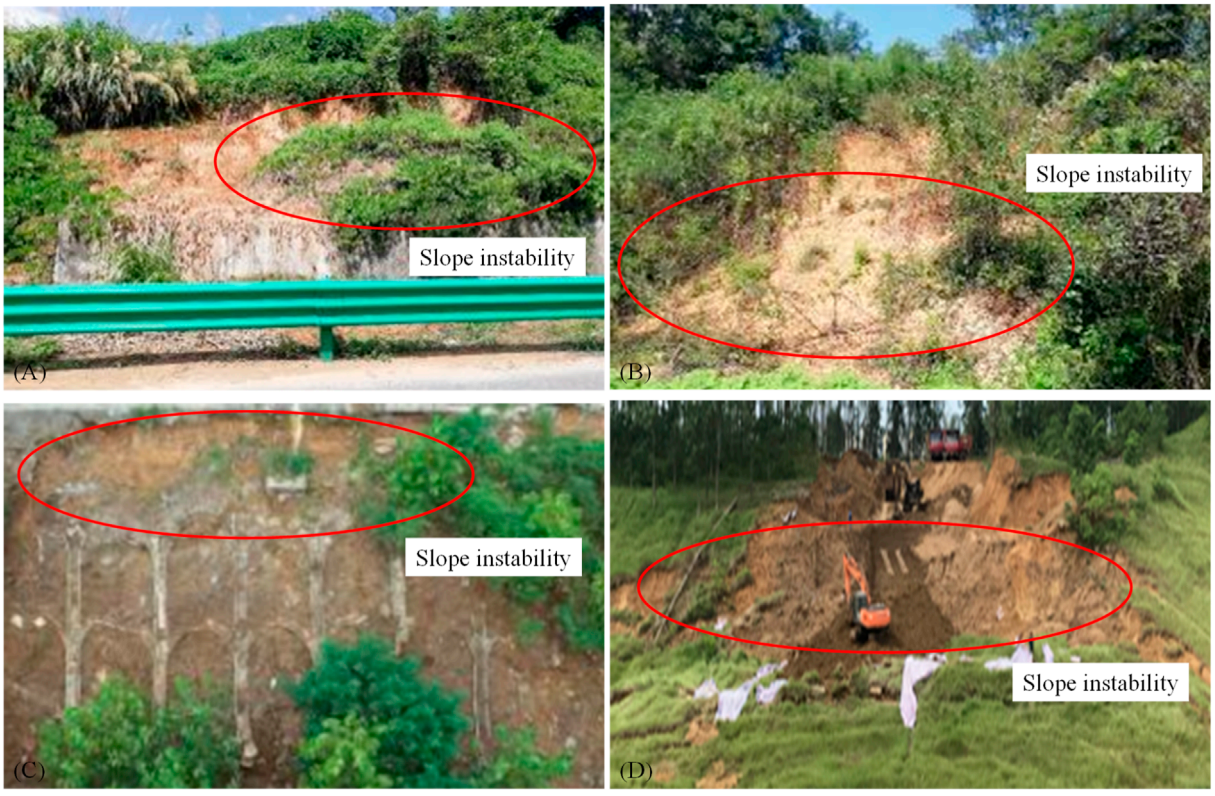

FIGURE 2
Slope instability along highways in the JiangHuai region.

conditions spanning 20 h, little deviation is observed between the slope's pore water pressure and initial distribution, suggesting minimal penetration of rainwater into the slope surface, primarily flowing down the slope.

As depicted in Figures 6, 7, under rainstorm conditions and following 5 h of rainfall, pore water pressure distribution across the slope expands irrespective of the slope rate employed. This expansion indicates rainwater penetration through the ecological control and water-resistant structures of the expansive soil. However, for rainstorm durations shorter than 4 h, the "storage-blocking" water control ecological prevention and control technology noticeably delays rainwater infiltration. Conversely, under light

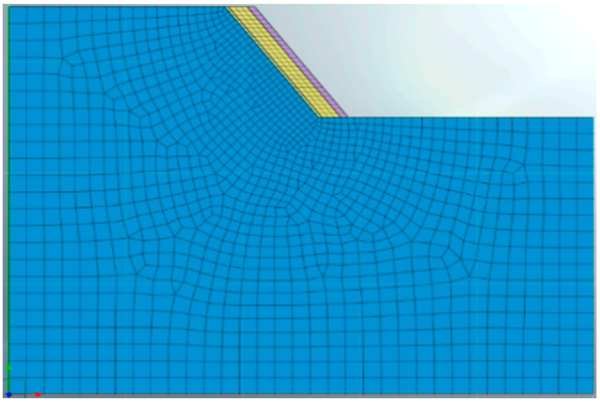

FIGURE 3
Rainfall calculation model.

rainfall, the ecological protection structure of the expansive soil slope remains intact, effectively stabilizing the slope's moisture. The "storage-blocking" ecological control technology proves suitable for the predominantly light rainfall conditions of the JiangHuai region but may necessitate adjustment in response to extreme rainstorms.

3.3 Slope deformation analysis

Figures 8, 9 display the vertical displacement change cloud diagrams of the slope during rainfall. Interestingly, regardless of rainstorm or light rainfall conditions, the deformation cloud diagrams exhibit a similar pattern. Slopes reinforced with expansive soil ecological control technology depict shallow circular arcs on the sliding surface during rainfall, suggesting effective prevention of water infiltration into the slope's interior. Maximum deformation occurs at the foot of the slope, with deformation gradually decreasing towards the top of the soil body. In engineering practice, reinforcing the foot of expansive soil slopes is crucial to mitigate deformation.

As depicted in Figure 10, a comparison of slope safety coefficients reveals that without reinforcement measures, the stability coefficient of expansive soil slopes falls below 1.5. Conversely, the utilization of expansive soil ecological control technology significantly enhances overall slope stability. Regardless of the slope rate, the stability coefficient exceeds 3, far surpassing the critical landslide threshold. This underscores the effectiveness of expansive soil ecological control technology in bolstering expansive soil slope stability. However, under rainstorm conditions, the slope stability coefficient is lower than that under light rainfall. This discrepancy arises from the intense rainfall exceeding the saturated permeability coefficient, allowing rainwater to infiltrate the soil through slope fissures. Consequently, the slope undergoes rapid water erosion, resulting in shallow damage primarily along the slope surface.

4 Discussion

4.1 Moisture control mechanism of expansive soil slope

The effective management of weakly expansive soil slopes in the JiangHuai region hinges critically on the precise regulation of moisture in shallow-surface slopes. Given the correlation between suction and pore space in soil layers of varying grain sizes, an optimization approach for controlling weakly expansive soil slopes involves positing that the fine-grained and coarse-grained soil layers form a capillary blocking structure. Subsequently, the "storage-blocking" water effect of this capillary blocking structure is analyzed under rainfall-evaporation conditions, as depicted in Figure 11. In Figure 11A, the pore size of the fine-grained soil layer is uniformly small, with a thin layer of water present. Gravity's influence on this thin layer of water is disregarded, focusing instead on the equilibrium state of water within a single void, influenced by the vertical component of surface tension.

$$2\pi r_1 T + \pi r_1^2 P_t = 0 \tag{1}$$

Namely: $P_t = P_b = -2T/r_1$

Where: P_t and P_b represent the capillary pressure at the top and bottom surfaces of the thin layer of water, respectively; r_1 denotes the void radius of the fine-grained soil; and T represents the surface tension.

As water accumulates in the fine-grained soil layer (Figure 11B), gravity becomes significant, disrupting the mechanical equilibrium of the water column within the pore space and causing it to migrate downward into the lower coarse-grained soil layer under gravity's influence. When the water column reaches the interface between the fine and coarse-grained soil layers (Figure 11C), the aperture of the seepage channel alters, resulting in higher capillary pressure at the top of the water column compared to the bottom. This disparity in capillary pressure is utilized to counterbalance the gravitational force acting on the water column.

$$P'_t \pi r_1^2 = P'_b \pi r_2^2 + \gamma_w h_t A_w \tag{2}$$

Due to the minute radius of both the coarse- and fine-grained soil, as well as the rainwater column's area, the limiting height h_t corresponding to the critical state of capillary breakthrough can be simplified to:

$$h_t = (P'_t - P'_b)/\gamma_w \tag{3}$$

where: P'_t and P'_b represent the capillary pressure reaction forces at the top and bottom surfaces of the thin layer of water, respectively, with $P'_t = 2T/r_1$ and $P'_b = 2T/r_2$; r_2 denotes the radius of the void of the coarse-grained soil; γ_w signifies the rainwater heaviness; h_t denotes the rainwater infiltration height; and A_w represents the rainwater column area.

From Equation 3, it can be seen that the capillary blocking structure suction is regulated by controlling the compaction and grain size pore space to realize the role of water storage and blocking water infiltration of the fine-grained soil layer in the rainfall-evaporation process.

TABLE 1 Numerical simulation parameter values.

	Modulus of elasticity (kPa)	Bulk density (kN/m^3)	Poisson's ratio	Angle of internal friction (°)	Cohesion (kPa)
Ecological layer	15000	18.5	0.33	15.3	15.8
Fine-grained soil	45000	19.8	0.37	32.4	42.2
Coarse-grained soil	150000	20.0	0.35	36	0
Expansive soil	34000	19.6	0.28	17	23

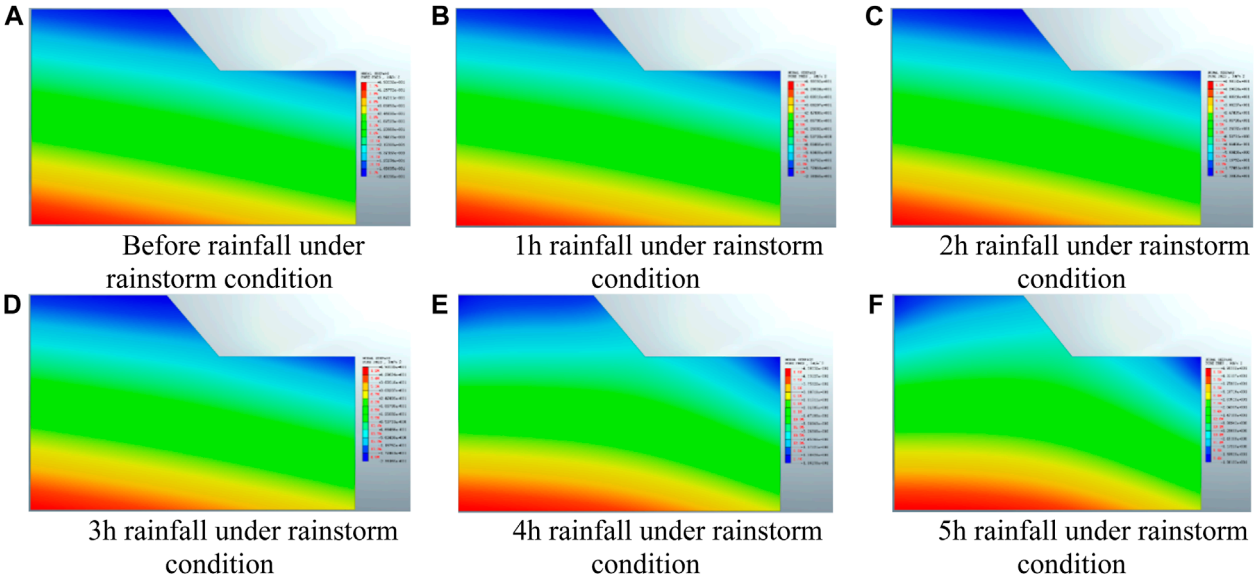

FIGURE 4
Distribution of pore water pressure duration under rainstorm conditions with a slope rate of 0.8. **(A)** Before rainfall under rainstorm condition. **(B)** 1 h rainfall under rainstorm condition. **(C)** 2 h rainfall under rainstorm condition. **(D)** 3 h rainfall under rainstorm condition. **(E)** 4 h rainfall under rainstorm condition. **(F)** 5 h rainfall under rainstorm condition.

If the water storage capacity of the fine-grained soil layer reaches its limit, this marks the failure of the capillary blocking structure. When the rainfall intensity is lower than the soil's percolation rate, the breakthrough time is primarily influenced by the intensity of rainfall.

$$t_b = \frac{h_t}{S\cos\theta} \tag{4}$$

where t_b denotes the failure time of the capillary blocking structure, θ represents the slope angle of the side slope, and S signifies the rainfall intensity.

When the rainfall intensity surpasses the percolation rate of the soil, surface runoff occurs. In this scenario, the breakthrough time is primarily influenced by the percolation properties of the soil.

$$t_b = \frac{h_t}{Q\cos\theta} = \frac{h_t \Delta L}{k_{sw}k_{rw}\cos\theta \Delta P} \tag{5}$$

where Q represents the rainfall flow rate, k_{sw} denotes the saturated permeability coefficient, and k_{rw} signifies the relative permeability coefficient. ΔP denotes the increment in driving force for soil infiltration, and ΔL represents the depth of soil infiltration per unit of water.

4.2 Analysis and discussion of influencing factors in ecological protection technology

The breakthrough time of the capillary barrier structure is crucial for ecological protection technology. When the breakthrough time exceeds the duration of rainfall, the ecological protection technology remains safe during precipitation. The breakthrough time of the capillary barrier structure is influenced by the thickness of the fine-grained soil layer, rainfall intensity, slope gradient, and the permeability coefficient of the soil. To determine the impact of each factor on ecological protection technology, a controlled variable method is used to perform parameter analysis on each factor individually. Specifically, the discussed parameter is treated as the variable, while the other parameters remain constant.

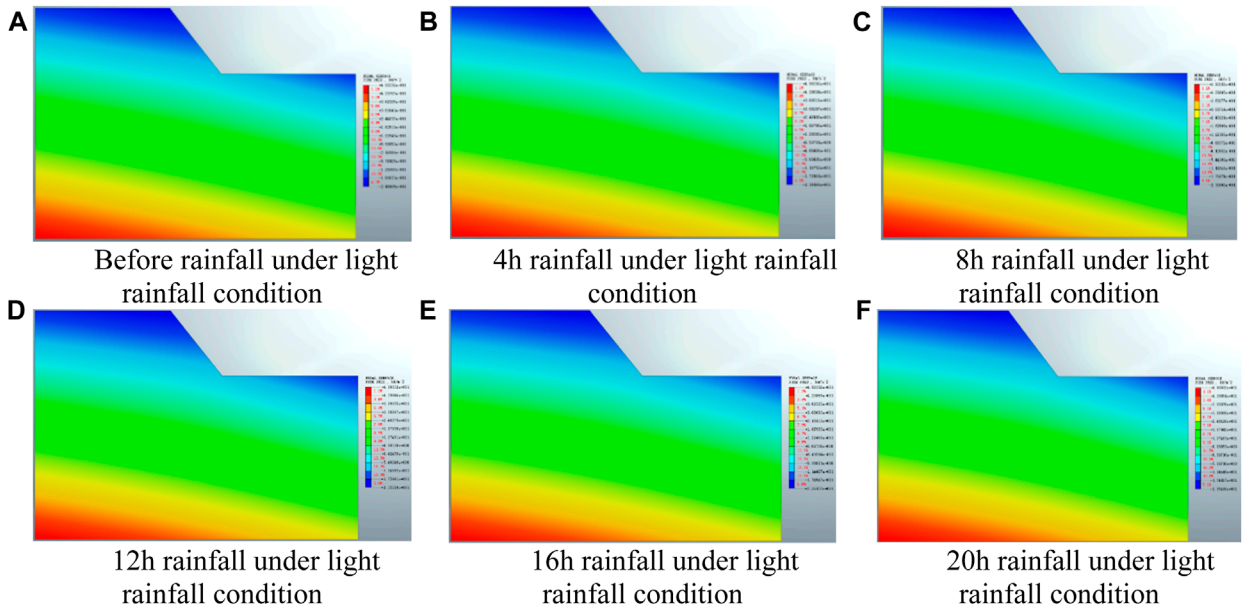

FIGURE 5
Distribution of pore water pressure duration under light rain conditions with a slope rate of 0.8. **(A)** Before rainfall under light rainfall condition. **(B)** 4 h rainfall under light rainfall condition. **(C)** 8 h rainfall under light rainfall condition. **(D)** 12 h rainfall under light rainfall condition. **(E)** 16 h rainfall under light rainfall condition. **(F)** 20 h rainfall under light rainfall condition.

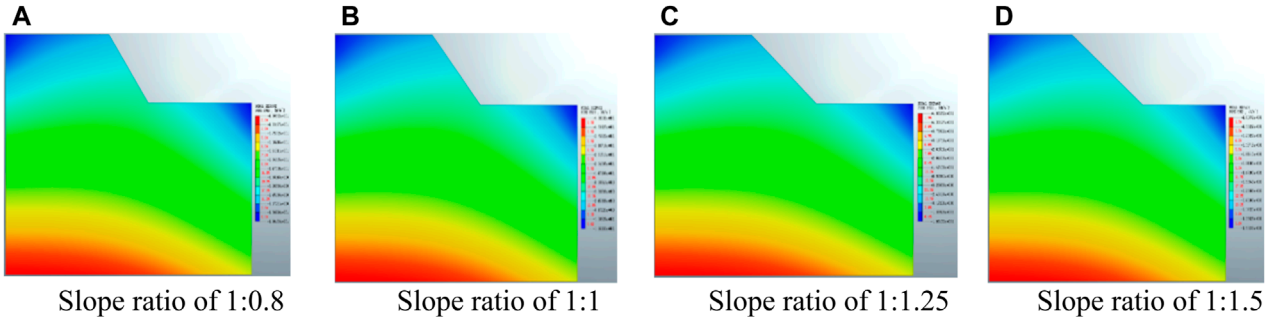

FIGURE 6
Pore water pressure distribution for rainstorm with different slope rates. **(A)** Slope ratio of 1:0.8. **(B)** Slope ratio of 1:1. **(C)** Slope ratio of 1:1.25. **(D)** Slope ratio of 1:1.5.

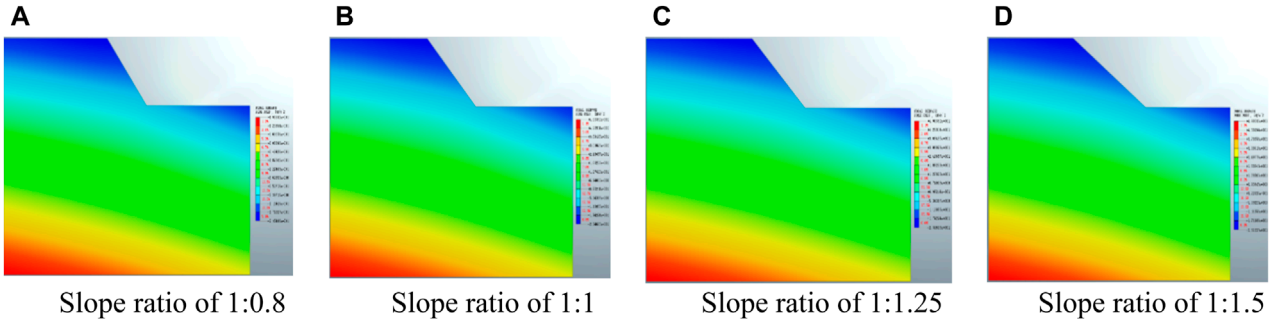

FIGURE 7
Pore water pressure distribution for light rain with different slope rates. **(A)** Slope ratio of 1:0.8. **(B)** Slope ratio of 1:1. **(C)** Slope ratio of 1:1.25. **(D)** Slope ratio of 1:1.5.

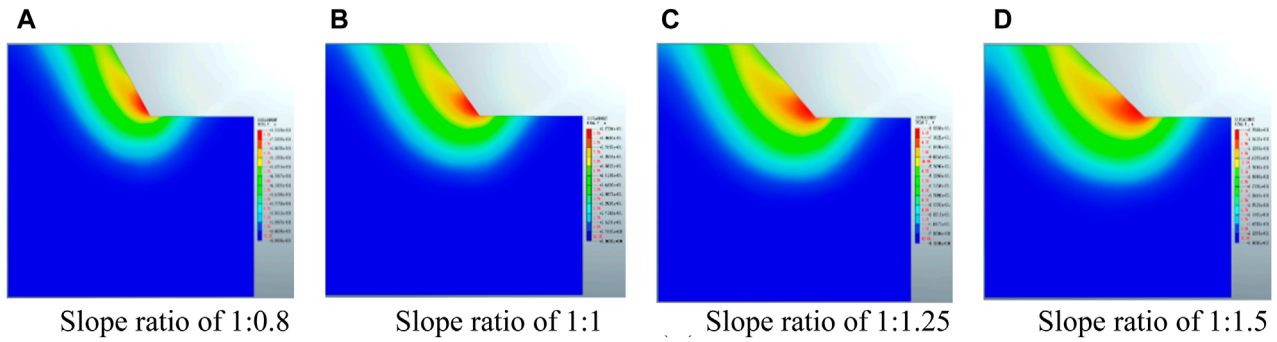

FIGURE 8
Slip surfaces of slopes with different slope rates under rainstorm conditions. **(A)** Slope ratio of 1:0.8. **(B)** Slope ratio of 1:1. **(C)** Slope ratio of 1:1.25. **(D)** Slope ratio of 1:1.5.

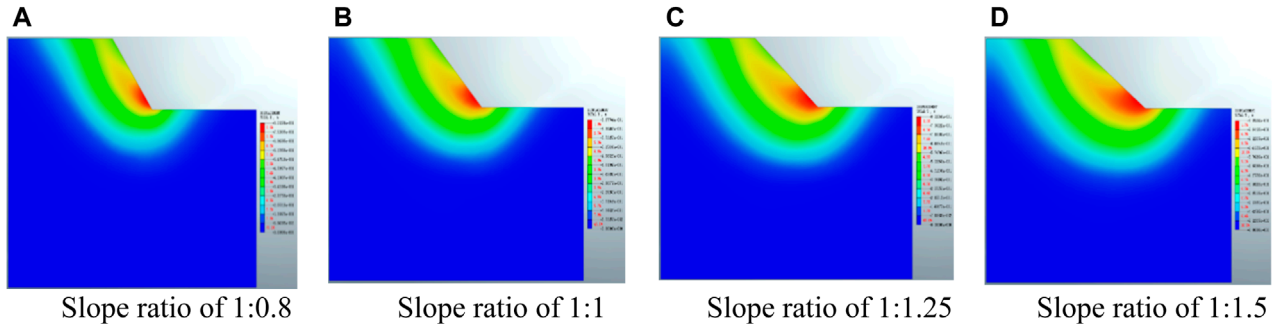

FIGURE 9
Slip surfaces of slopes with different slope rates under light rain conditions. **(A)** Slope ratio of 1:0.8. **(B)** Slope ratio of 1:1. **(C)** Slope ratio of 1:1.25. **(D)** Slope ratio of 1:1.5.

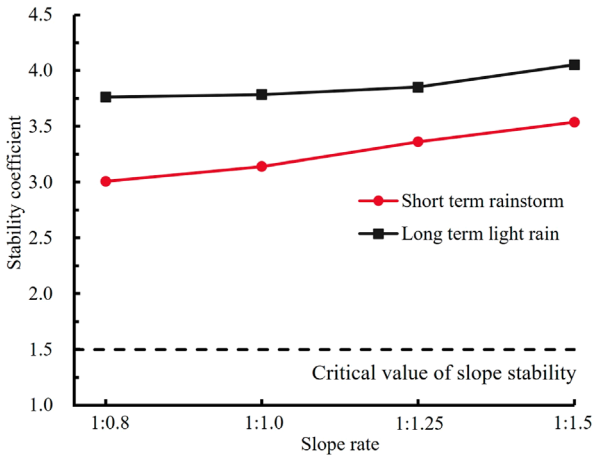

FIGURE 10
Stability coefficients of reinforced slopes under different operating conditions.

This approach is similar to controlling the variation of a single experimental parameter while keeping the other experimental parameters unchanged in an experiment.

The relationship between breakthrough time and the thickness of the fine-grained soil layer is derived through the parameter control variable method analysis of the thickness of the fine-grained soil layer in Equations 4, 5. The results are as follows:

$$t_b = C/h_t \tag{6}$$

When the rainfall intensity is less than the soil infiltration rate, $C=1/(S\cdot\cos\theta)$; when the rainfall intensity exceeds the soil infiltration rate, $C=\Delta L/(k_{sw}\cdot k_{rw}\cdot\cos\theta\cdot\Delta P)$. For different thicknesses of fine-grained soil, the remaining parameters are kept constant, and the value of C remains unchanged.

Equation 6 indicates that there is a positive correlation between the breakthrough time and the thickness of the fine-grained soil layer, as shown in Figure 12A. This finding is consistent with the research conducted by Li et al. (Li et al., 2022a; Li et al., 2022b) and Gao et al. (Gao et al., 2023)on the thickness of fine-grained soil layers. Figure 12B illustrates the relationship between the experimental values obtained by Li et al. and Gao et al. and the theoretical values from Equation 6 in this study, showing a similar linear relationship, with the C values of 155.03 and 105.67 and the R^2 values of 0.98 and 0.99, respectively. This indicates that regardless of whether the rainfall intensity is greater than the soil infiltration rate—whether

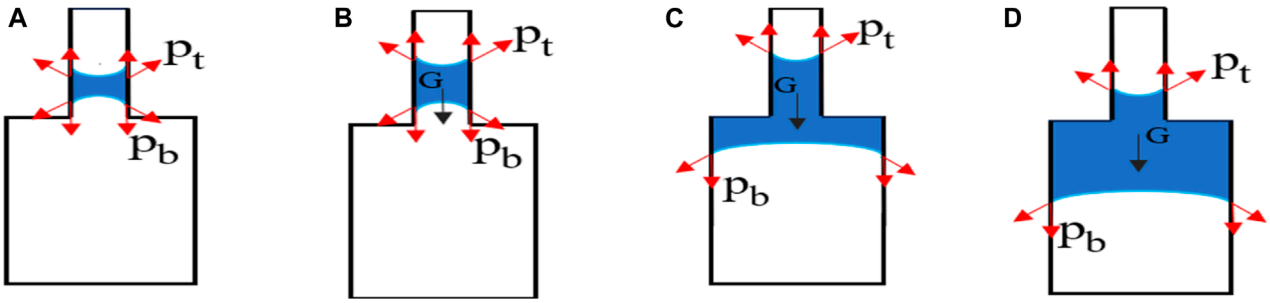

FIGURE 11
Mechanism of capillary blocking structure under rainfall conditions **(A–D)**.

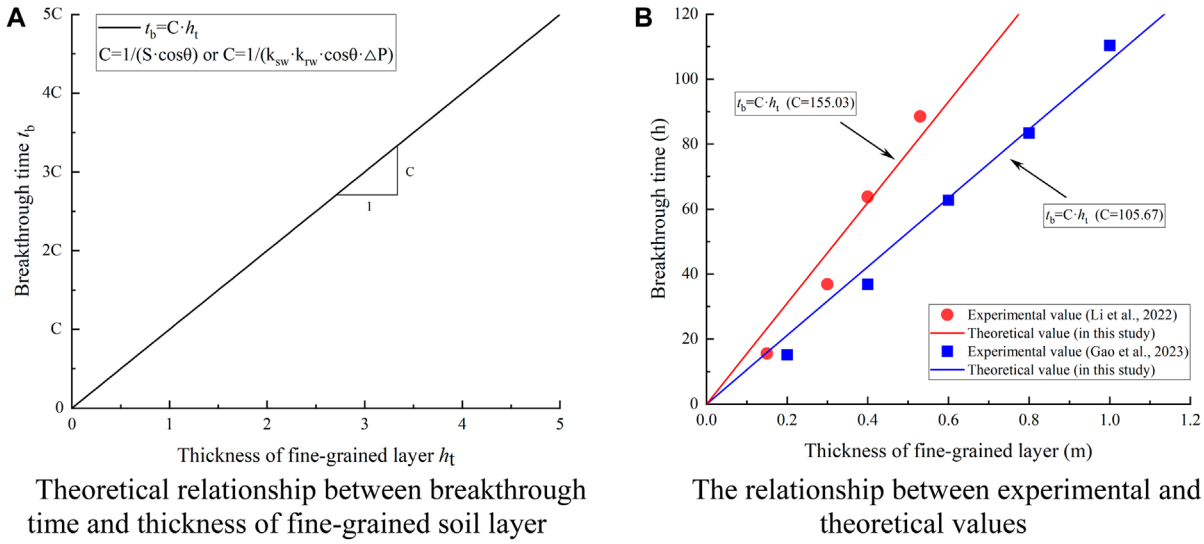

FIGURE 12
Relationship between breakthrough time and thickness of fine-grained soil layer. **(A)** Theoretical relationship between breakthrough time and thickness of fine-grained soil layer. **(B)** The relationship between experimental and theoretical values.

during short-term heavy rain or prolonged light rain—the breakthrough time is positively influenced by the thickness of the fine-grained soil layer. Increasing the thickness can extend the breakthrough time.

Additionally, the thickness of the fine-grained soil layer affects the evaporation process during the rainfall-evaporation cycle. Excessive soil thickness is detrimental to the evaporation of moisture within the soil layer and the restoration of its anti-seepage function after the rainfall ends (Li et al., 2022a; Wang et al., 2022). Research has shown that the initial state of the fine-grained soil layer has a significant impact on the performance of the capillary barrier (Li et al., 2013). When the cover soil is initially moist, its effectiveness cannot be guaranteed, as water can easily infiltrate into the underlying soil layers. By ensuring that the breakthrough time exceeds the rainfall duration during the rainfall process and the anti-seepage function is restored during the evaporation process, selecting an appropriate thickness for the fine-grained soil layer can reduce construction costs.

By analyzing the rainfall intensity, the relationship between breakthrough time and rainfall intensity is obtained as follows:

$$t_b = C/S \quad (7)$$

When the rainfall intensity is less than the soil infiltration rate, $C=h_t/\cos\theta$. For different rainfall intensities, with all other parameters kept constant, the value of C remains unchanged.

Equation 7 shows a negative correlation between rainfall intensity and the thickness of the fine-grained soil layer, as depicted in Figure 13A. This finding is consistent with the research conducted by Li et al. (Li et al., 2022a; Li et al., 2022b) on rainfall intensity. Figure 13B illustrates the relationship between the experimental values obtained by Li et al. and the theoretical values from Equation 7 in this study, demonstrating the same power function relationship, with the C value of 901.44 and the R^2 values of 0.98. This indicates that when the rainfall intensity is less than the soil infiltration rate, the breakthrough time is negatively impacted by the rainfall intensity—the greater the rainfall intensity, the shorter the breakthrough time.

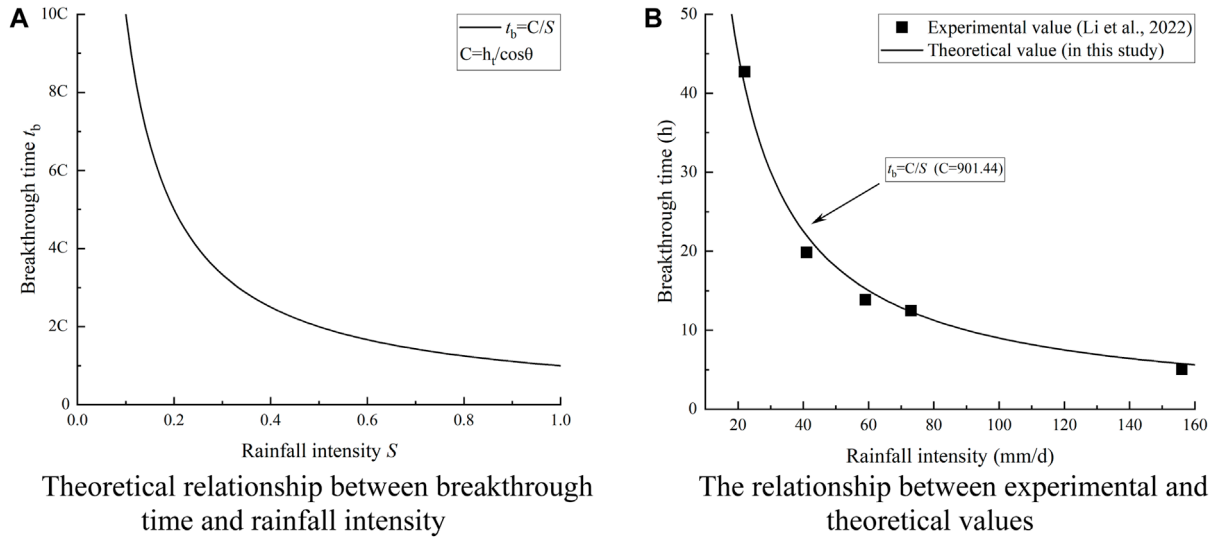

FIGURE 13
Relationship between breakthrough time and rainfall intensity. **(A)** Theoretical relationship between breakthrough time and rainfall intensity. **(B)** The relationship between experimental and theoretical values.

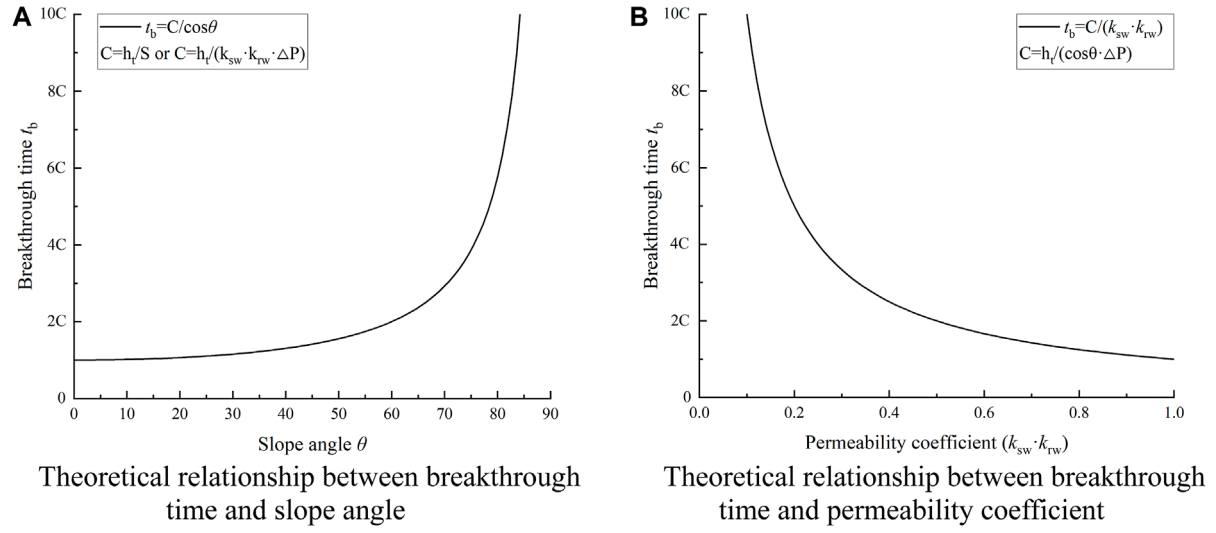

FIGURE 14
The relationship between breakthrough time and slope angle and permeability coefficient. **(A)** Theoretical relationship between breakthrough time and slope angle. **(B)** Theoretical relationship between breakthrough time and permeability coefficient.

Furthermore, the power function relationship between breakthrough time and rainfall intensity suggests that the degree of impact of rainfall intensity changes on breakthrough time is related to the current rainfall intensity. In the graph, this is shown by the breakthrough time decreasing rapidly at first and then more slowly as rainfall intensity increases. This aligns with the observation that when rainfall intensity exceeds the soil infiltration rate, the breakthrough time is primarily influenced by the soil's infiltration properties rather than rainfall intensity. When designing slopes, the possibility of rainfall intensities exceeding normal levels must be considered (Jiao et al., 2023a; Jiao et al., 2023b). Extreme rainfall can lead to a rapid decrease in breakthrough time, resulting in actual breakthrough times significantly lower than the expected design values, especially in regions with typically low rainfall intensities.

By analyzing the slope angle, the relationship between breakthrough time and slope angle is obtained as follows:

$$t_b = C/\cos\theta \tag{8}$$

When the rainfall intensity is less than the soil infiltration rate, C = h_t/S; when the rainfall intensity exceeds the soil infiltration rate, C

$= \Delta L \cdot h_t/(k_{sw} \cdot k_{rw} \cdot \Delta P)$. For different rainfall intensities, with all other parameters kept constant, the value of C remains unchanged.

Equation 8 indicates a positive correlation between breakthrough time and slope angle, as shown in Figure 14A. The greater the slope angle, the longer the breakthrough time, suggesting that increasing the slope angle helps extend the breakthrough time of the capillary barrier. This finding is consistent with the studies by Li et al. (Li et al., 2013) and Qian et al. (Qian et al., 2010), which observed that the efficiency of the capillary barrier increases with the slope angle.

However, while the slope angle affects the breakthrough time of the capillary barrier, it also influences the stability of the slope itself. When the slope angle is too steep, the stability of the slope decreases (Gao et al., 2022; Guo et al., 2024). Notably, compared to other factors, the impact of the slope angle on the capillary barrier varies with location. Research indicates that the breakthrough time of the capillary barrier is shortest at the toe of the slope and longest at the crest (Li et al., 2013). Similarly, in this study, numerical models showed that the maximum deformation of the slope occurs at the toe, with soil deformation decreasing towards the crest. This is related to the infiltration water in the upper fine-grained soil layer (crest) being diverted to the lower part of the cover system (toe) (Gao et al., 2022).

In general, increasing the slope angle can enhance lateral water movement, thereby extending the breakthrough time of the cover layer. However, if the water cannot drain from the capillary barrier, the diverted water will accumulate at the toe, causing a breakthrough. Therefore, it is necessary to promptly discharge the infiltrated water retained in the fine-grained layer and maintain good drainage conditions at the toe to ensure the long-term stability of the capillary barrier (Li et al., 2023). Based on this, lateral drainage facilities were installed in sections of the slope in this study, with water collection facilities set up at the toe.

By analyzing the permeability coefficient, the relationship between breakthrough time and permeability coefficient is obtained as follows:

$$t_b = C/(k_{sw} \cdot k_{rw}) \tag{9}$$

When the rainfall intensity exceeds the soil infiltration rate, $C = h_t/(\cos\theta \cdot \Delta P)$. For different permeability coefficients, with all other parameters kept constant, the value of C remains unchanged.

Equation 9 shows a negative correlation between breakthrough time and permeability coefficient, as illustrated in Figure 14B. The smaller the permeability coefficient, the longer the breakthrough time. This indicates that to extend the breakthrough time of the capillary barrier, materials with a lower permeability coefficient can be selected for the fine-grained soil layer. Moreover, as one of the key design parameters for the fine-grained soil layer, choosing an appropriate lower permeability coefficient can meet the design objectives for breakthrough time while reducing the thickness of the fine-grained soil layer, leading to lower engineering costs and easier practical construction. However, the permeability coefficient should not be too low, considering the water needs for the normal growth of ecological layer plants and the transpiration of vegetation (Guo et al., 2022; Jiao et al., 2023b). Additionally, an excessively thin fine-grained soil layer can also pose practical construction challenges.

The analysis and discussion of the influencing factors of ecological protection technology indicate that in engineering practice, reasonable selection and coordinated optimization of various parameters of the protection technology can achieve more economical and sustainable solutions while extending the breakthrough time of ecological protection technology. Furthermore, in addition to improvements in influencing factors, ecological protection techniques can be coupled with geosynthetics, protective layers with lower permeability coefficients, and unsaturated conductive drainage layers in order to improve protection against climate extremes (Ng et al., 2019; Ng et al., 2022; Ma et al., 2023; Ng et al., 2023; Bian et al., 2024b; Bian et al., 2024c).

4.3 Application and assessment analysis of ecological protection technologies

Based on the mechanism of capillary retention, the "storage-retention" water-control ecological prevention and control technology for expansive soil slopes, which has the functions of both capillary retention and root soil fixation, was proposed and tested in a designated section of the HeLiuYe Expressway. This test section features a slope height of 6.08 m and a length of 20 m, with a slope ratio of 1:1.5. The "storage-blocking" moisture control ecological prevention and control technology primarily comprises ecological layer, fine-grained layer, coarse-grained layer, and drainage geogrid. The coarse-grained layer predominantly consists of sand and gravel, while the fine-grained layer comprises silt or clay material. Positioned atop the fine-grained layer, the ecological layer absorbs a portion of rainwater during rainfall. Furthermore, the fine-grained soil supplies water to the vegetation during dry periods. Drainage geogrid serve as a support framework for the capillary retention layer on the slope and provide rainwater evacuation channels for rainfall, as illustrated in Figure 15. Specific arrangement plan; the slope surface from bottom to top are coarse-grained layer, geotextile, fine-grained layer and ecological layer respectively. The thickness of the coarse-grained layer is 5 cm, and gravel with a grain size of 10–50 mm is used as the material. The thickness of the fine-grained layer is 25 cm, and powdered soil with a particle size of not more than 2 mm is used as the material. The top of the pulverized soil is covered with cultivated soil and vegetation as an ecological layer. The anchored drainage cell consists of uniformly distributed cells, each containing a prefabricated geocell (C30) to provide strength support and drainage holes to provide slope drainage. The cells have a side length of 2.5 m and are embedded in the soil with dimensions of 260 mm x 300 mm, while the exposed portion is designed as a drainage trench.

In the "storage-blocking" moisture control ecological prevention and control technology, the fine-grained layer and the coarse-grained layer, as well as the coarse-grained layer and the expansive soil body, collectively constitute a double-layer chain capillary blocking structure. During rainfall conditions, the fine-grained layer serves to impede water infiltration, while concurrently, in conjunction with the coarse-grained layer, it establishes a capillary blocking effect, retaining water within the fine-grained layer. Should moisture breach the fine-grained layer, the coarse-grained layer facilitates drainage of water from the slope side to the drain or foot of the slope. Similarly, during

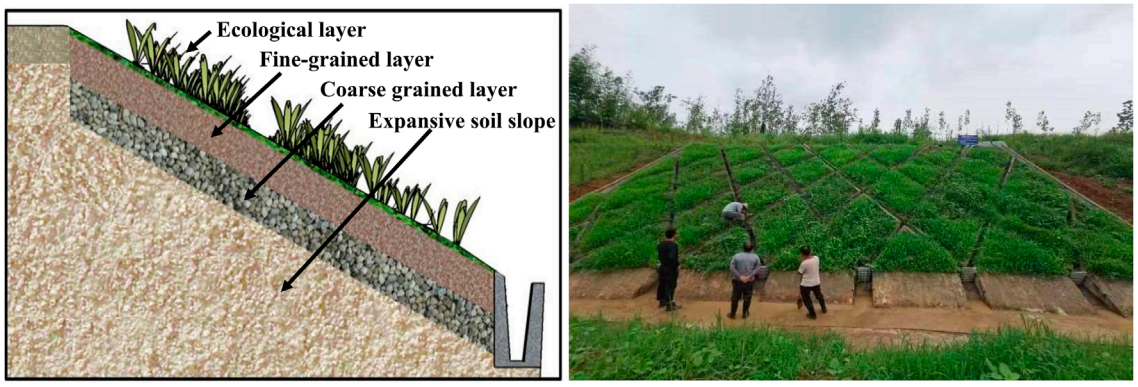

FIGURE 15
Effectiveness of the test section.

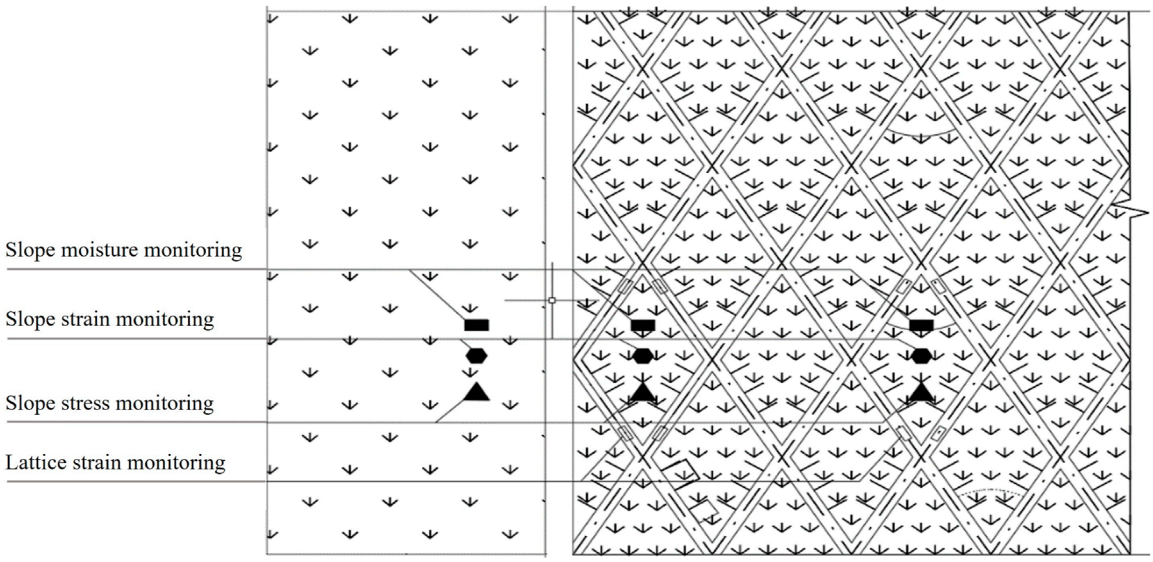

FIGURE 16
Monitoring layout.

TABLE 2 Weather changes in early October 2022.

Date	10.1	10.2	10.3	10.4	10.5	10.6	10.7
Weather	Cloudy	Sunny	Cloudy	Light rain	Moderate rain	Moderate rain	Light rain
Maximum/Minimum Temperature (°C)	35/25	38/26	38/16	17/12	12/9	13/10	16/11

dry seasons and evaporation conditions, moisture within the expansive soil slope evaporates upwards during transportation. This process forms a capillary blocking effect between the expansive soil body and the coarse-grained layer. The capillary pressure difference balances the gravitational force of the moisture between the layers, thereby preventing water loss from the expansive soil body.

To assess the effectiveness and long-term stability of expansive soil slopes, a monitoring system was installed at the demonstration site. This system utilizes TDR (time-domain reflectometers) to monitor water transport within the expansive soil, soil pressure boxes to monitor slope soil pressure, and strain gauges to monitor slope strain. Simultaneously, identical monitoring units were deployed at corresponding depths on adjacent primary

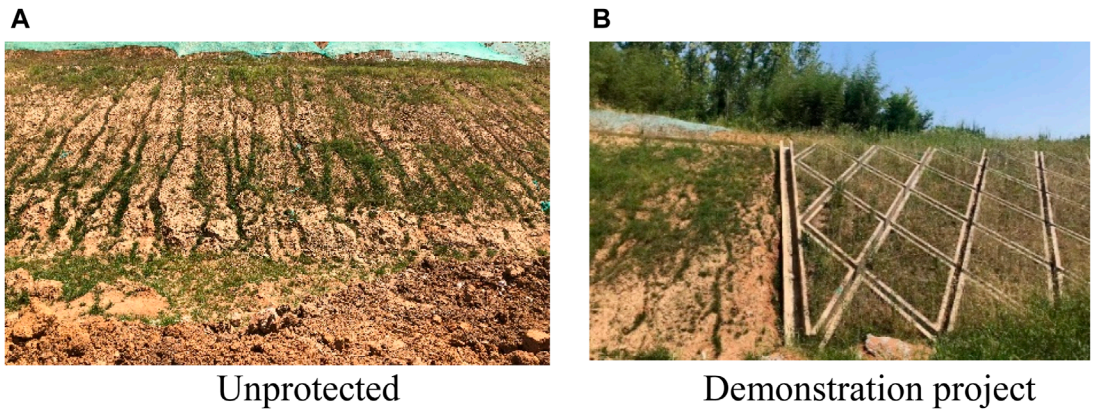

FIGURE 17
Comparison of deformation between the demonstration project and the unprotected site. **(A)** Unprotected. **(B)** Demonstration project.

slopes to facilitate a comparative analysis of slope control effectiveness. The arrangement scheme of the monitoring system is shown in Figure 16. The monitoring cell consists of a soil moisture sensor, an embedded strain gauge and a soil pressure cell. The monitoring units are deployed in the grid cell at the boundary of the designed slope and another grid cell spaced apart from it. In the depth direction, two sets of monitoring units were installed in the pulverized clay layer, and one set of monitoring units was installed in the expansive soil slope, with depths of 150 mm, 250 mm, and 500 mm, respectively, and the same monitoring units were installed at the same depths in the adjacent primary slopes to compare the effectiveness of the slope control. Embedded strain gauges were placed at the boundaries of the selected lattice units, one at each of the four boundaries, to monitor the strain of the U-shaped lattice during concrete placement.

Table 2 presents the weather conditions in early October 2022. It indicates that the weather was sunny from October 1 to October 3, followed by continuous rainfall from October 4 to October 7. Through on-site observation and comparison between the demonstration slopes equipped with ecological control technology for expansive soil and the unprotected slopes, several key findings were noted. The deformation of the unprotected slopes unfolded across three stages: (I) shallow traction deformation; (II) creep deformation during the infiltration-evaporation stage; and (III) onset of continuous light rainfall, where initial appearance of expansion and contraction fissures remained shallow, and the intensity of light rainfall did not surpass the saturated permeability coefficient, thereby resulting in no noticeable runoff generation on the expansive soil slope. However, as the rainfall duration increased, transient saturation of the soil around the fissures gradually formed, leading to sheet erosion and mudflow damage on the slope. Subsequently, the middle section of the slope beneath the surface layer gradually saturated, and hauling the top of the slope shoulder along the gully appeared creeping and sliding misalignment, the slippery surface continued to deepen. Loose soil continued to slide, with fine-grained mudflow converging at the foot of the slope. Following cessation of rainfall and subsequent evaporation, creeping deformation of the soil resulted in the formation of contraction cracks, tension cracks at the slope top, and numerous mesh cracks along the slope. These cracks served as advantageous channels for runoff during subsequent rainfall, thereby contributing significantly to the continued instability of the expansive soil slope in later stages. Figure 17 illustrates the comparison between the demonstration project site and the unprotected deformation. From the figure, it can be seen that the surface of the unprotected slopes has formed significant cracks under the rainfall-evaporation cycle, while the surface of the slopes with the protection technology has not changed significantly. This reflects the stability of the slope brought about by the ecological protection technique and also shows the ongoing damage to the unprotected slope. During the rainfall-evaporation cycle, soils on the surface of unprotected expansive soil slopes will experience fissure development and rainwater erosion (Ma et al., 2023). Studies have shown that moisture changes are a key factor in the development of soil fissures (Liu et al., 2023). During evaporation, the topsoil loses moisture and shrinks, creating tensile stresses between particles. When the tensile stress is greater than the tensile strength of the soil, cracks will develop. During rainfall, water enters deeper inside the soil along the cracks. In addition, the soil particles formed by the broken soil body will be carried away by the runoff from the slope, and then the erosion area and soil loss will gradually increase. The amount of vegetation on the two slopes also showed significant differences. At the beginning of the field test, both side slopes were arranged with surface vegetation as shown in Figure 15. After the rainfall-evaporation cycle, the amount of vegetation on the slope surface of the unprotected slope decreased significantly, while the amount of vegetation on the surface of the slope with the protection technique remained intact. It was shown that the vegetation root system has a significant inhibitory effect on crack development in expansive soils, in addition to the fact that vegetation on the slope surface of the side slope can reduce infiltration by utilizing evapotranspiration (Ng et al., 2019; Ng et al., 2022) (Cao et al., 2023; Xu et al., 2023). Unprotected slopes will lose large amounts of soil due to slope fracture development and rainfall erosion. This will make it difficult to maintain normal plant growth and the slope will be deprived of vegetation protection.

Figure 18 illustrates the changes in moisture and soil pressure at the test section site from October 1 to 7. Weather conditions were hot from October 1 to 3, during which the moisture content

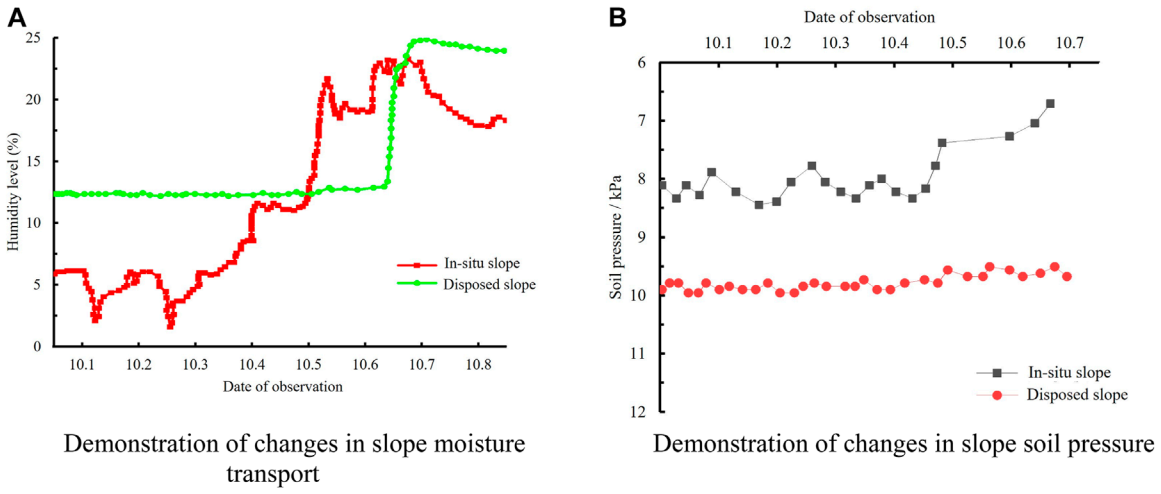

FIGURE 18
Demonstration project site moisture and soil pressure monitoring data. **(A)** Demonstration of changes in slope moisture transport. **(B)** Demonstration of changes in slope soil pressure.

of the original slope remained at approximately 6%. About 24 h after the onset of rainfall, evident moisture increase in the soil body of the original slope was observed, with moisture levels rising to about 22% around October 4. Correspondingly, soil pressure within the original slope body commenced increasing around October 4, aligning with the results of numerical simulation. Despite the added weight due to the construction of the ecological protection layer, the treated slope maintained an *in situ* humidity of 12%. At the onset of rainfall on October 4, the treated slope exhibited minimal changes in moisture content. However, by October 7, infiltration of rainfall through the ecological protection unit was evident, leading to a significant increase in slope moisture content, resembling that of the original slope. Nonetheless, soil pressure did not increase, indicating that approximately 70 h of continuous rainfall allowed partial penetration of the toughness ecological protection unit, effectively delaying the ingress of rainwater into the slope. In addition, it can be seen from the monitoring in the field that the moisture and earth pressure inside the unprotected slopes changed significantly when the outside environment changed. Even when there is no rainfall outside, the daytime and nighttime temperatures will significantly affect the moisture inside the expansive soil slopes, resulting in changes in earth pressure. On the contrary, the water and earth pressure inside the slope with ecological protection technology can be stabilized for a long time. This indicates that the ecological protection technology effectively reduces the sensitivity of expansive soil slopes to the external environment.

As a special kind of widely distributed soil, expansive soil is very sensitive to changes in the external environment due to the hydrophilicity of its constituent minerals and its obvious expansion and contraction. In human production and living activities, they are often threatened by geologic disasters caused by the destabilization of expansive soil slopes. As shown in Figures 2C, D, landslides still occurred after the slope protection of expansive soil slopes, indicating that the traditional slope management methods have long-term stability problems in the protection of expansive soil slopes. This is attributed to the lack of resilience of the traditional slope protection methods in terms of protection capacity, and the lack of resilience of the protection set up from minor damage to total collapse under the long-term effects of the environment. The ecological control technology of expansive soil slope used in this study has the recovery ability of anti-seepage function, which provides a guarantee for the long-term maintenance of the effect of expansive soil slope management in the actual project. In addition, the eco-control technology of expansive soil slopes also has obvious practical benefits in terms of construction cost and environmental friendliness. The less restrictive types of coarse and fine particles used in the construction project and the wide range of sources for obtaining them bring lower construction costs in the actual project. The introduction of ecological layer of vegetation brings more prominent protection and recovery ability, but also can carry out carbon dioxide capture and reduce soil erosion and loss, which brings additional ecological benefits (Bian et al., 2024d). Therefore, the ecological control technology of expansive soil slopes has the advantages of long-term stability, low cost, and environmental friendliness in dealing with the threat of geologic hazards caused by the destabilization of expansive soil slopes in the project of stabilization of expansive soil slopes in the JiangHuai area.

In summary, the ecological control technique for expansive soil slopes effectively prevented rainwater infiltration, especially under light rainfall conditions, with sustained blocking capacity. These findings suggest that the eco-control technique for expansive soil slopes can effectively regulate slope moisture changes and is effective in enhancing the stability of expansive soil slopes. The discussion and validation of the feasibility, sustainability, and protective effects of the ecological slope control technology in this study can help provide researchers and design engineers in the field of geology and engineering with sustainable new ways to cope with the geohazards of expansive soil slope instability and to reduce the geohazard risks of expansive soil slope instability. It is important to note that there is still much room for improvement in the ability of ecological

control techniques to cope with extreme storms. The existence of extreme climate may be the main reason limiting the large-scale popularization and application of ecological control technology in a wider area. Therefore, the protective ability of ecological control technology for expansive soil slopes under extreme rainstorm conditions is further investigated and improved by looking at the influencing factors of ecological slope protection technology.

5 Conclusion

Based on theoretical analysis, numerical simulation, and on-site testing methods, the following conclusions can be drawn about the ecological prevention and control technology of "storage resistance" water regulation in expansive soil slopes in the JiangHuai River.

(1) Leveraging the mechanism of capillary water transport, the ecological protection technology for expansive soil slopes, centered on toughness ecological protection and reinforced with drainage geogrids, was innovated. This technology amalgamates capillary blocking and root consolidation functionalities, effectively managing water dynamics within the slope and curtailing fissure development in expansive soil slopes.

(2) During rainfall events, the shallow-surface toughness eco-protection unit on expansive soil slopes employs the fine-grained layer to impede water infiltration. Simultaneously, aided by the capillary blocking effect created by the fine-grained and coarse-grained layers, water is retained within the fine-grained layer. Should water breach the fine-grained layer, the coarse-grained layer facilitates lateral water transport towards the drainage channel or the slope's base.

(3) In evaporative conditions, as water within the expansive soil slope evaporates during transportation, a capillary blocking effect is formed between the expansive soil body and the coarse-grained layer. This effect effectively prevents water loss from the expansive soil body.

(4) The ecological protection scheme for expansive soil slopes effectively manages pore water pressure distribution and notably prolongs rainwater infiltration time. During rainstorm events lasting less than 4 h, the expansive soil slope remains stable. Similarly, under light rainfall conditions persisting for 20 h, the "surface-shallow-deep" ecological protection layer of the expansive soil slope remains intact.

(5) In practical engineering applications, reinforcing the support at the slope's base is necessary within the expansive soil slope support plan. By selecting and optimizing the technical parameters, it is possible to achieve a more economical and sustainable solution while extending the protection time.

Data availability statement

The original contributions presented in the study are included in the article/supplementary material, further inquiries can be directed to the corresponding author.

Author contributions

WT: Data curation, Investigation, Writing–review and editing. YW: Validation, Writing–review and editing. XB: Writing–original draft. ZR: Visualization, Writing–review and editing. LX: Methodology, Software, Writing–review and editing. FW: Resources, Writing–review and editing. HZ: Supervision, Writing–review and editing.

Funding

The author(s) declare that financial support was received for the research, authorship, and/or publication of this article. This study is supported by the National Natural Science Foundation of China (Grant Nos. 52178328, 42377190).

Conflict of interest

Authors WT and FW were employed by Anhui Transport Consulting and Design Institute Co. Ltd. Author YW was employed by East China Electric Power Design Institute Co., Ltd.

The remaining authors declare that the research was conducted in the absence of any commercial or financial relationships that could be construed as a potential conflict of interest.

The reviewer JJ declared a shared affiliation with the authors XB, ZR to the handling editor at time of review.

Publisher's note

References

Bian, X., Peng, W. H., Qiu, C. C., Xu, G. Z., and Yao, Y. K. (2023). Model test on bearing capacity of cemented slurry reinforced pile composite foundation. *Case. Stud. Constr. Mater.* 19, e02482. doi:10.1016/j.cscm.2023.e02482

Bian, X., Fan, Z. Y., Liu, J. X., and Li, X. Z. (2024a). Regional 3D geological modelling along metro lines based on stacking ensemble model. *Undergr. Space* 18, 65–82. doi:10.1016/j.undsp.2023.12.002

Bian, X., Ren, Z. L., Zeng, L. L., Yao, Y. K., Zhao, F. Y., and Li, X. Z. (2024b). Effects of biochar on the compressibility of soil with high water content. *J. Clean. Prod.* 434, 140032. doi:10.1016/j.jclepro.2023.140032

Bian, X., Zhao, F. Y., Zeng, L. L., Ren, Z. L., and Li, X. Z. (2024c). Role of superabsorbent polymer in compression behavior of high-water-content slurries. *Acta Geotech.*, 1–16. doi:10.1007/s11440-024-02296-x

Bian, X., Gao, Z. Y., Zhao, P., and Li, X. Z. (2024d). uantitative analysis of low carbon effect of urban underground space in Xinjiekou district of Nanjing city, China. *Tunnelling Underground Space Technol.* 143, 105502. doi:10.1016/j.tust.2023.105502

Cai, W. C., Lan, F., Huang, X. H., Hao, J. F., Xia, W. F., Tang, R., et al. (2024). Generative probabilistic prediction of precipitation induced landslide deformation with variational autoencoder and gated recurrent unit. *Front. Earth Sci.* 12, 1394129. doi:10.3389/feart.2024.1394129

Cai, Z. Y., Chen, H., Huang, Y. H., and Zhang, C. (2019). Failure mechanism of canal slopes of expansive soils considering action of wetting-drying cycles. *Chin. J. Geotechnical Eng.* 41 (11), 1977–1982 (In Chinese). doi:10.11779/CJGE201911001

Cao, T. T., Zhang, H. O., Chen, T. Q., Yang, C. X., Wang, J., Guo, Z., et al. (2023). Research on the mechanism of plant root protection for soil slope stability. *Plos one* 18 (11), e0293661. doi:10.1371/journal.pone.0293661

Chang, J., Yang, H. P., Xiao, J., Chen, G. Y., Ma, H. F., and Chen, Q. (2021). Fissure development law and micro-mechanism of Baise expansive soil under wet-dry cycles of acid rain. *China J. Highw. Transp.* 34 (1), 47–56 (In Chinese). doi:10.19721/j.cnki.1001-7372.2021.01.005

Deng, M. J., Cai, Z. Y., Zhu, X., and Zhang, C. (2020). Failure mechanism and reinforcement measures of shallow slopes of expansive soils in Northern Xinjiang. *Chin. J. Geotechnical Eng.* 42 (S2), 50–55 (In Chinese). doi:10.11779/CJGE2020S2009

Ding, W. T., and Lei, S. Y. (2010). Triaxial tests on reinforced expansive soil under different reinforced modes. *Rock and Soil Mech.* 31 (4), 1147–1150 (In Chinese). doi:10.16285/j.rsm.2010.04.044

Duan, S. L., Xu, G. Y., Dong, J. G., and Qian, H. Y. (2019). Deformation characteristic of expansive soil under wet-dry cycles. *J. Xi'an Univ. Sci. Technol.* 39 (5), 819–825 (In Chinese). doi:10.13800/j.cnki.xakjdxxb.2019.0511

Feng, Y. R., Yang, W. Q., Wan, J., and Li, H. J. (2023). Granular risk assessment of earthquake induced landslide via latent representations of stacked autoencoder. *Front. Environ. Sci.* 11, 1308808. doi:10.3389/fenvs.2023.1308808

Gao, C., Ye, W. M., Lu, P. H., Liu, Z. R., Wang, Q., and Chen, Y. G. (2023). An infiltration model for inclined covers with consideration of capillary barrier effect. *Eng. Geol.* 326, 107318. doi:10.1016/j.enggeo.2023.107318

Gao, C., Zhu, Y. M., and Zhang, Y. W. (2022). Stability analysis of the inclined capillary barrier covers under rainfall condition. *Buildings* 12 (8), 1218. doi:10.3390/buildings12081218

Gong, B. W., and Tong, J. (2009). Application of geosynthetic in expansive rock canal slope treatment in south to north water transfer project. *J. Yangtze River Sci. Res. Inst.* 26 (11), 81. (In Chinese).

Gong, B. W., Xu, X. T., and Hu, B. (2023). Ecological treatment of the channel in expansive soil section of the Water diversion project from the Yangtze to Huaihe River. *South-to-North Water Transfers Water Sci. Technol.* 21 (5), 1006–1012 (In Chinese). doi:10.13476/j.cnki.nsbdqk.2023.0096

Guo, H. W., Ng, C. W. W., Zhang, Q., Chen, R., and Zhang, Y. M. (2022). Effects of plant growth on water infiltration into three-layer landfill cover system. *J. Eng. Geol.* 30 (5), 1731–1743 (In Chinese). doi:10.13544/j.cnki.jeg.2022-0406

Guo, H. W., Ng, C. W. W., Zhang, Q., Qu, C. X., and Hu, L. W. (2024). Modelling the water diversion of a sustainable cover system under humid climates. *J. Rock Mech. Geotechnical Eng.* 16, 2429–2440. doi:10.1016/j.jrmge.2023.10.017

Guo, Z., and Zhao, Z. (2021). Numerical analysis of an expansive subgrade slope subjected to rainfall infiltration. *Bull. Eng. Geol. Environ.* 80 (7), 5481–5491. doi:10.1007/s10064-021-02274-7

Hu, M. J., Kong, L. W., Guo, A. G., and Liu, G. S. (2007). Expansive soil embankment stability and geogrid treatment effect analysis with strength zoning method. *Rock Soil Mech.* 28 (9), 1861–1865 (In Chinese). doi:10.16285/j.rsm.2007.09.006

Hu, Y. N., Ji, J., Sun, Z. B., and Dias, D. (2023). First order reliability-based design optimization of 3D pile-reinforced slopes with Pareto optimality. *Comput. Geotechnics* 162, 105635. doi:10.1016/j.compgeo.2023.105635

Ji, J., Cui, H. Z., Zhang, T., Song, J., and Gao, Y. F. (2022). A GIS-based tool for probabilistic physical modelling and prediction of landslides: GIS-FORM landslide susceptibility analysis in seismic areas. *Landslides* 19 (9), 2213–2231. doi:10.1007/s10346-022-01885-9

Ji, J., and Wang, L. P. (2022). Efficient geotechnical reliability analysis using weighted uniform simulation method involving correlated nonnormal random variables. *J. Eng. Mech.* 148 (6), 06022001. doi:10.1061/(asce)em.1943-7889.0002101

Jiao, W. G., Lin, C. S., Tu, B., He, M. W., Liu, Z. N., and Zhang, Y. (2023b). Evaluation of long-term anti-seepage performance of capillary barrier cover in semi humid area and analysis on meteorological mechanism of percolation. *China Civ. Eng. J.* 56 (10), 118–126 (In Chinese). doi:10.15951/j.tmgcxb.22050482

Jiao, W. G., Tuo, B., Zhang, S., He, M. W., Lin, C. S., and Liu, Z. N. (2023a). Anti-seepage performance verification and analysis of high-risk permeable meteorological period of capillary barrier cover in Northwest non humid area. *Rock Soil Mech.* 44 (S1), 539–547 (In Chinese). doi:10.16285/j.rsm.2022.1075

Kong, L. W., and Chen, Z. H. (2012). Advancement in the techniques for special soils and slopes. *China Civ. Eng. J.* 45 (5), 141–161 (In Chinese). doi:10.15951/j.tmgcxb.2012.05.001

Li, J. H., Du, L., Chen, R., and Zhang, L. M. (2013). Numerical investigation of the performance of covers with capillary barrier effects in South China. *Comput. Geotechnics* 48, 304–315. doi:10.1016/j.compgeo.2012.08.008

Li, X. K., Li, X., Wang, F., Liu, A. Q., Liu, L., and Liu, Y. (2022b). Experimental study on water storage capacity and breakthrough time of capillary barrier cover. *Chin. J. Rock Mech. Eng.* 41 (7), 1501–1511 (In Chinese). doi:10.13722/j.cnki.jrme.2021.0839

Li, X. K., Li, X., Wang, F., and Liu, Y. (2022a). The design criterion for capillary barrier cover in multi-climate regions. *Waste Manag.* 149, 33–41. doi:10.1016/j.wasman.2022.06.002

Li, X. K., Li, X., Wu, Y., and Gao, L. (2023). A novel unsaturated drainage layer in capillary barrier cover for slope protection. *Bull. Eng. Geol. Environ.* 82 (4), 108. doi:10.1007/s10064-023-03093-8

Liu, H. Q., and Yin, Z. Z. (2010). Test study of influence of crack evolution on strength parameters of expansive soil. *Rock Soil Mech.* 31 (3), 727–731 (In Chinese). doi:10.16285/j.rsm.2010.03.032

Liu, X. Y., Wu, Q. H., Xu, L. H., and Zhuang, Y. F. (2023). A novel double-layer system for infiltration control and improvement in the stability of expansive soil slopes. *Int. J. Geosynth. Ground Eng.* 9 (1), 4. doi:10.1007/s40891-023-00425-2

Ma, S. K., He, B. F., Ma, M., Huang, Z., Chen, S. J., and Yue, H. (2023). Novel protection systems for the improvement in soil and water stability of expansive soil slopes. *J. Mt. Sci.* 20 (10), 3066–3083. doi:10.1007/s11629-023-8178-3

MWR (Ministry of Water Resources the People's Republic of China) (2019). *Standard for geotechnical testing method. GB/T 50123-2019*. Beijing: MWR.

Ng, C. W. W., Guo, H. W., Ni, J. J., Chen, R., Xue, Q., Zhang, Y. M., et al. (2022). Long-term field performance of non-vegetated and vegetated three-layer landfill cover systems using construction waste without geomembrane. *Géotechnique* 74 (2), 155–173. doi:10.1680/jgeot.21.00238

Ng, C. W. W., Lu, B. W., Ni, J. J., Chen, Y. M., Chen, R., and Guo, H. W. (2019). Effects of vegetation type on water infiltration in a three-layer cover system using recycled concrete. *J. Zhejiang Univ. Sci. A* 20 (1), 1–9. doi:10.1631/jzus.a1800373

Ng, C. W. W., Ng, C. L., Ni, J. J., Guo, H. W., Zhang, Q., Xue, Q., et al. (2023). Analysis of a landfill cover without geomembrane using varied particle sizes of recycled concrete. *J. Rock Mech. Geotechnical Eng.* 15 (5), 1263–1273. doi:10.1016/j.jrmge.2022.09.004

Pei, P., Zhao, Y., Ni, P., and Mei, G. (2020). A protective measure for expansive soil slopes based on moisture content control. *Eng. Geol.* 269, 105527. doi:10.1016/j.enggeo.2020.105527

Qian, T. W., Huo, L. J., and Zhao, D. Y. (2010). Laboratory investigation into factors affecting performance of capillary barrier system in unsaturated soil. *Water, Air, Soil Pollut.* 206 (1-4), 295–306. doi:10.1007/s11270-009-0106-9

Song, Y. Q., Yang, Y. H., Cheng, K., and Xu, H. Y. (2023). Summary of ecological bank protection structure in Anhui section of Yangtze-to-Huaihe water diversion project. *Port Waterw. Eng.* (08), 70–76+113 (In Chinese). doi:10.16233/j.cnki.issn1002-4972.20230803.017

Wang, N. X., Zhang, W. M., Gu, X. W., and Zeng, Y. (2008). Lateral swelling pressure of expansive soil acting on retaining wall due to inundation. *J. Hydraulic Eng.* 39 (5), 580–587 (In Chinese). doi:10.13243/j.cnki.slxb.2008.05.017

Wang, S. Y., Liu, A. H., Zou, J. Q., Wu, Z. Z., and Zhang, W. (2022). Review on slope protection technique of capillary barrier. *Yangtze River* 53 (4), 79–85+97 (In Chinese). doi:10.16232/j.cnki.1001-4179.2022.04.013

Wang, X. U., Tian, C., Huang, L. L., and Fan, J. Z. (2016). Study of stability analysis method for expansive soil with fissures. *Nat. ence J. Xiangtan Univ.* 38 (1), 27–32 (In Chinese). doi:10.13715/j.cnki.nsjxu.2016.01.006

Wang, Z., Qiu, Z. Q., Cai, S. T., Hu, H. L., Cui, B. J., and Lu, Y. (2007). A case history of application of FRP screw anchor and geosynthetics in repairing of canal slope of expansive soils. *South-to-North Water Transfers Water Sci. Technol.* 5 (5), 127–131 (In Chinese). doi:10.13476/j.cnki.nsbdqk.2007.05.014

Wei, B. X., Chen, L. S., Xiao, L. M., Zheng, W., and Bai, Y. X. (2021). Unsaturated seepage analysis of expansive soil slope under rainfall infiltration based on multi-field coupling. *J. Yangtze River Sci. Res. Inst.* 38 (3), 90 (In Chinese). doi:10.11988/ckyyb.20200006

Xian, S. H., Xu, Y. Z., Yao, H. L., Lu, Z., and Dong, C. (2017). Model test study of constraint to deformation of expansive soil by anchor reinforced vegetation system. *Rock Soil Mech.* 38 (S1), 158–166 (In Chinese). doi:10.16285/j.rsm.2017.S1.018

Xu, Y. F. (2020). Hydraulic mechanism and swelling deformation theory of expansive soils. *Chin. J. Geotechnical Eng.* 42 (11), 1979–1987 (In Chinese). doi:10.11779/CJGE202011002

Xu, Y. Z., Guo, Y. Y., Huang, Z., Liu, D. Z., Huang, Q. N., and Tang, H. (2023). Study on Cynodon dactylon root system affecting dry–wet cracking behavior and shear strength characteristics of expansive soil. *Sci. Rep.* 13 (1), 13052. doi:10.1038/s41598-023-39770-7

Yang, H. P., Wang, J., Zhan, W. T., and Li, Y. Y. (2011). Study of treatment technology and design scheme of expansive soil subgrade for Nanning outer ring expressway. *Rock Soil Mech.* 32 (S2), 359–365 (In Chinese). doi:10.16285/j.rsm.2011.s2.057

Zhang, R., Lan, T., Zheng, J. L., and Gao, Q. F. (2024). Field performance of a geogrid-reinforced expansive soil slope: a case study. *Bull. Eng. Geol. Environ.* 83 (1), 7. doi:10.1007/s10064-023-03478-9

Zhang, R., Long, M. X., Lan, T., Zheng, J. L., and Geoff, C. (2020). Stability analysis method of geogrid reinforced expansive soil slopes and its engineering application. *J. Central South Univ.* 27 (7), 1965–1980. doi:10.1007/s11771-020-4423-x

Zhang, R., Long, M. X., and Zheng, J. L. (2019). Comparison of environmental impacts of two alternative stabilization techniques on expansive soil slopes. *Adv. Civ. Eng.* 2019 (1), 9454929. doi:10.1155/2019/9454929

Zhang, R., Tang, P. X., Lan, T., Liu, Z. J., and Ling, S. G. (2022). Resilient and sustainability analysis of flexible supporting structure of expansive soil slope. *Sustainability* 14 (19), 12813. doi:10.3390/su141912813

Zheng, J. J., Lu, S. Q., and Cao, W. Z.(2017). Numerical analysis of mechanical and deformation characteristics of composite rigid-flexible anti-slide pile. *J. Huazhong Univ. Sci. Technol. Nat. Sci. Ed.* 45(4), 39–44. (In Chinese). doi:10.13245/j.hust.170408

Zhou, B. S., Wang, B. T., Zhang, H. X., Wang, Y. H., and Kang, J. Y. (2016). Stability analysis of expansive soil slopes based on integral rigid-body equilibrium method. *Geotechnics* 37 (S2), 525–532 (In Chinese). doi:10.16285/j.rsm.2016.S2.067